

HST NICMOS Imaging of the Planetary-mass Companion to the Young Brown Dwarf 2MASSWJ 1207334–393254

Inseok Song¹, G. Schneider², B. Zuckerman³, J. Farihi¹, E. E. Becklin³, M. S. Bessell⁴,
P. Lowrance⁵, B. A. Macintosh⁶

ABSTRACT

Multi-band (0.9 to 1.6 μm) images of the TW Hydrae Association (TWA) brown dwarf, 2MASSWJ 1207334–393254 (also known as 2M1207), and its candidate planetary mass companion (2M1207b) were obtained on 2004 Aug 28 and 2005 Apr 26 with HST/NICMOS. The images from these two epochs unequivocally confirm the two objects as a common proper motion pair (16.0σ confidence). A new measurement of the proper motion of 2M1207 implies a distance to the system of 59 ± 7 pc and a projected separation of 46 ± 5 AU. The NICMOS and previously published VLT photometry of 2M1207b, extending overall from 0.9 to 3.8 μm , are fully consistent with an object of a few Jupiter masses at the canonical age of a TWA member (~ 8 Myr) based on evolutionary models of young giant planets. These observations provide information on the physical nature of 2M1207b and unambiguously establish that the first direct image of a planetary mass companion in orbit around a self-luminous body, other than our Sun, has been secured.

Subject headings: (stars:) planetary systems — stars: low-mass, brown dwarfs — stars: individual (2MASSWJ 1207334–393254)

¹Gemini Observatory, Northern Operations Center, 670 North A‘ohoku Place, Hilo, HI 96720, USA, song@gemini.edu, jfarihi@gemini.edu

²Steward Observatory, The University of Arizona, 933 N. Cherry Ave., Tucson, AZ 85721 USA, gschneider@as.arizona.edu

³Dept. of Physics & Astronomy and Center for Astrobiology, University of California, Los Angeles, 475 Portola Plaza, Los Angeles, CA 90095–1547, USA, ben@astro.ucla.edu, becklin@astro.ucla.edu

⁴Research School of Astronomy and Astrophysics, Institute of Advanced Studies, The Australian National University, ACT 2611, Australia, bessell@mso.anu.edu.au

⁵Spitzer Science Center, Infrared Processing and Analysis Center, MS 220-6, Pasadena, CA 91125, USA, lowrance@ipac.caltech.edu

⁶I Division, Lawrence Livermore National Laboratory, 7000 East Avenue, Livermore, CA 94550, bmac@igpp.ucllnl.org

1. Introduction

Beginning in 2004 July, with HST/NICMOS, we initiated a systematic imaging search for extra-solar gas giant planets around 116 young nearby stars and brown dwarfs. These targets are $\lesssim 50$ Myr old and located within 60 pc of Earth, making them among the best known targets for such a survey (Zuckerman & Song 2004).

A brown dwarf in the ~ 8 Myr old TW Hydrae Association, 2MASSWJ 1207334–393254 (Gizis 2002; hereafter 2M1207), was included in our HST target list and its observation was planned for 2005 April. However, on 2004 Apr 27 (UT), 2M1207 was observed with VLT/NACO and a faint companion candidate was discovered $\sim 0''.78$ from the brown dwarf (Chauvin *et al.* 2004). NICMOS observations of 2M1207 were replanned and brought forward to 2004 August. The resulting NICMOS photometric data, shorter in wavelength than could be obtained with adaptive optics on the VLT, support the conjecture that 2M1207b is of mid- to late-L type based upon its color indices. With the limited precision of the proper motion data then available for 2M1207 and the short time between the VLT and 2004 August HST observations, common proper motion with 2M1207b was established at the 2.6σ level (Schneider *et al.* 2004). Additional observations were obtained with the VLT during 2005 February and March that much more precisely demonstrated common proper motion between 2M1207 and its companion (Chauvin *et al.* 2005a). As described in Section 4.1, the proper motion value of 2M1207 (Scholz *et al.* 2005) used in Chauvin *et al.* (2005a) was not well measured, causing the analysis to be somewhat over-optimistic.

With the higher accuracy HST astrometry and a new, more accurate, proper motion measurement of 2M1207 in the present paper, we report a more definitive common proper motion between 2M1207 and 2M1207b. We also present short near-IR wavelength diagnostic photometry which cannot currently be obtained from the ground given the performance limitations of adaptive optics imaging.

2. HST Observations

HST near-IR observations of 2M1207 were obtained with NICMOS camera 1 (~ 43 mas/pixel) at two observational epochs: 2004 Aug 28 and 2005 Apr 26. At each epoch, 2M1207 was observed at two field orientations (spacecraft roll angles) in successive HST orbits to permit self-subtractions of the rotationally invariant PSF, thereby significantly increasing the visibility of the nearby companion. Direct imaging in camera 1, rather than coronagraphy in camera 2, was planned due to the $\sim 0''.78$ angular separation of 2M1207 and its putative planetary-mass companion and the relatively benign contrast ratios expected based on the

VLT observations. NICMOS camera 1 provides shorter wavelength diagnostic filters than camera 2 with a commensurately finer pixel scale to permit critical sampling of the PSF at short near-IR wavelengths. Details of the NICMOS observations are listed in Table 1.

Raw multiaccum frames were converted to count-rate images with an IDL-based analog to the STSDAS CALNICA task, using calibration reference files developed by the NICMOS Instrument Definition Team and the Space Telescope Science Institute. Known defective pixels (under-responsive due to particulate contamination, and those with excessive dark currents) were replaced by two-dimensional Gaussian weighted interpolation of good neighbor pixels (with wavelength dependent weighting radii of the PSF FWHM for the filters employed). Dark subtracted, linearity-corrected, flat-fielded, cosmic ray rejected count-rate images were post-processed to remove additional well-characterized detector artifacts. For each filter in each visit, the four images were astrometrically registered to the position of the first image. Position offsets were taken as reported in the downlinked spacecraft telemetry, through the CD matrices in the science data file headers, and verified by Gaussian profile fitting and image centroiding of the 2M1207 PSF image cores. Image registration was accomplished via sinc function apodized bicubic interpolation, rebinning the interpolated images into a two times finer spatially resampled grid. Then, images were median combined to create better sampled, higher S/N, and defect minimized count-rate images suitable for PSF subtraction and of high photometric fidelity. Details of the data calibration and processing methodologies are discussed in Schneider et al. (2005).

2.1. Photometry

Photometry of 2M1207b was carried out after reducing the light of the primary star by subtracting the dither combined image at the second field orientation from the first. This roll subtraction virtually eliminated the spatially variable light from the primary outside of $0''.2$, leaving a positive and negative image of 2M1207b displaced by the differential field rotation. Since the PSFs of the companion partially overlap in this difference image, model PSFs were created to fit and null out actual image PSFs separately by adjusting position and flux density. This created an image at each orientation with the primary removed and only one companion remaining. These two images of the companion were then rotated by the appropriate spacecraft roll angle and combined (Figure 1). The model PSFs were created using TinyTim 6.1a (Krist & Hook 1997), which produces high fidelity filter and position dependent model PSFs for HST instruments.

The in-band flux densities (and Vega system magnitudes) of 2M1207 were established from the unsubtracted, dither combined images resulting from each orbit independently. To

verify the model PSF subtraction method used to determine the companion magnitudes, we measured the primary magnitudes both with flux-scaled model PSF subtraction, and with background subtracted aperture photometry (corrected to an infinite aperture).

The measured F090M and F160W magnitudes at the two NICMOS epochs are consistent (Table 2), and flux-weighted mean apparent magnitudes from both epoch measurements are $m_{F090M} = 22.46 \pm 0.25$ mag and $m_{F160W} = 18.26 \pm 0.02$ mag, respectively.

2.2. Astrometry

The NICMOS camera 1 pixel scales applicable to both epochs of our 2M1207 observations are: X scale = 43.190 mas/pixel, Y scale = 43.016 mas/pixel. The median combined calibrated count rate images were geometrically corrected to yield flux-conserved resampled pixels of 43.190 mas/pixel in both axes. All astrometric measures were made on the geometrically corrected images.

The location of the primary was measured from the combined image by Gaussian profile fitting of the primary’s PSF core. We also measured the position of a serendipitously appearing field star, which could be used for future epoch differential proper motion measures of 2M1207 itself (Table 3).

The locations of the companion, one from each field orientation at each epoch, were determined by the position offsets of the model PSF implants used to null the companion images. The relative positions of 2M1207 and its companion were transformed to position angle (PA; degrees east of north) and angular separation (in mas) based upon the well established HST/NICMOS focal plane metrology (aperture orientation in the telescope focal plane), the celestial orientation of the spacecraft, and the detector X/Y image scales of NICMOS camera 1.

3. 2M1207 Color Indices and Implications

In Figure 2a, $m_{F090M} - m_{F160W}$ and $m_K - m_L$ colors of 2M1207 and b (Table 2) are compared to those of model calculations – “Dusty model” [Chabrier *et al.* 2000] and “Clear model” [Baraffe *et al.* 2003] – and field M, L, and T dwarfs from Leggett *et al.* (2002). Our red colors are consistent with Chauvin *et al.* (2004) who noted 2M1207b has a very red color ($m_H - m_K = 1.16$ mag) even compared to most known L dwarfs. Our colors for 2M1207b fall in between two extreme model cases indicating that dust clouds significantly affect its atmosphere. AB Pic b, a ~ 13 Jupiter mass (M_J) young planetary (or brown dwarf)

companion to the ~ 30 Myr old K2V star, AB Pic (Chauvin *et al.* 2005b), also has unusually red near-IR colors for an L1 dwarf (Figure 2b). A field L-dwarf, 2MASS J01415823–4633574, with very low surface gravity also shows very red near-IR colors (Kirkpatrick *et al.* 2006). In each of these cases, the unusual redness of these objects must be related to low surface gravity due to youth and this extreme red color can be used to identify young brown dwarfs in the solar neighborhood.

With our estimated distance of 59 ± 7 pc (see Section 5), F090M & F160W absolute magnitudes imply a mass of $2 - 8 M_J$ for 2M1207b (“Dusty” model: $5 - 8 M_J$ and “Clear” model: $2 - 5 M_J$). On the other hand, the best estimated mass of 2M1207b from a color-color diagram (Figure 2a) is $6 - 8 M_J$. From these mass ranges, the mass of 2M1207b is estimated to be $5 \pm 3 M_J$ and the temperature corresponding to this mass range is $920 - 1540$ K. Our estimated mass is consistent with the earlier estimate by Chauvin *et al.* (2004) from HKL’ photometric data ($5 \pm 2 M_J$) which was based on a larger distance (70 pc). The fact that we derive the same estimated mass with a smaller distance indicates that 2M1207b is brighter at shorter wavelengths (e.g., F090M) than model predictions which implies a bluer $m_{F090M} - m_{F160W}$ color than expected. Unusually red $m_H - m_K$ and blue $m_{F090M} - m_{F160W}$ colors could indicate that 2M1207b is somewhat subluminescent in the H (F160W) band compared to models and to field L dwarfs.

4. Confirmation of Physical Companionship

4.1. Improved Proper Motion Determination of 2M1207

Scholz *et al.* (2005) estimated the proper motion¹ of 2M1207 as, $(\mu_\alpha, \mu_\delta) = (-78 \pm 11, -24 \pm 9)$ mas/yr, using positions from SuperCOSMOS, 2MASS, and DENIS catalogs and from the Chandra database. As there are large differences in the accuracy between the SuperCOSMOS, 2MASS, and DENIS positions (e.g., < 60 mas for 2MASS versus < 500 mas for SuperCOSMOS), a precise and reliable estimation of proper motion was difficult to obtain (Mamajek 2005). Mamajek (2005) estimated proper motions of 2M1207 ($\mu_\alpha = -72 \pm 7, \mu_\delta =$

¹We note that two notations are used in the literature for proper motions in the RA direction; μ_α and $\mu_\alpha \cos \delta$. While it is true that the number of arc seconds to go once around in RA changes as a function of declination (so the need of the $\cos \delta$ term), that is all that changes. Offsets, proper motions, etc given in arc second are not dependent on declination. Therefore, it is not necessary or even correct to use a notation $\mu_\alpha \cos \delta$ for proper motions given in arc second per year as in Hipparcos, Tycho-2, UCAC2, etc. Here we follow precedent as well established by Gliese (1969) in his Catalog of Nearby Stars, and list proper motions in arc seconds per year.

-22 ± 9) mas/yr using positions from the same set of catalogs as in Scholz *et al.* (2005) excepting the problematic Chandra pointing position. Mamajek’s calculation takes into account the positional errors of input catalog positions and his derived proper motions are overlapping, within errors, with our proper motion measurements described below. However, as discussed in Section 5, there are some caveats with respect to the analysis by Mamajek (2005).

A more precise measurement of 2M1207’s proper motion was obtained in the following manner. On 2005 Mar 2, a single 120 second exposure I_C -band image of the field surrounding 2M1207 was obtained at a parallactic angle of 44.15° utilizing the Tektronix 2048×2048 CCD camera on the University of Hawaii 2.2 meter Telescope at Mauna Kea Observatory. The measured FWHM of point sources in the frame was $1''.1$ (5 pixels). An archival image, observed on 1978 May 2, was retrieved from the SuperCOSMOS Sky Survey database, where a digitized scan was extracted from a UK Schmidt Telescope plate. Because the I_C -band frame was obtained through high airmass (3.3) and 2M1207 is considerably redder than other objects in the frame, differential atmospheric refraction could affect the estimated proper motions (Monet et al. 1992). The IRAF task SYNPHOT was used to calculate the shift in effective wavelength between a typical field star (average G8) and 2M1207 (M8), resulting in a 175\AA shift in the Cousins I -band filter. At the observed elevation of 17.7° , this shift from 7890\AA to 8065\AA yields a differential refraction of ≈ 50 mas (Howell 2000) which is small compared to the centroid shift of ~ 1800 mas over 27 years. Moreover, Howell’s calculation is for an altitude of 2.2 km whereas our measurement was done at an altitude of 4.1 km, thus the true differential atmospheric refraction effect should be smaller than 50 mas.

About sixty point sources were selected within the common $7'.5 \times 7'.5$ field of view of the I_C -band image and the 1978.33 SuperCOSMOS image. These point sources have centroids that are measured with robust S/N ($\gtrsim 10$, unsaturated) and without obvious proper motion when blinking with the 2005 I_C -band image. The centroid coordinates of the sources together with those of 2M1207 were entered into the IRAF routine GEOMAP which calculates a general coordinate transformation, including rotation and distortion. The deviation (while excluded from the calculation) of 2M1207 from the resulting coordinate transformation should be its relative motion with respect to the field sources, whose residuals give a measurement of the standard error. The resulting proper motion of 2M1207 is calculated to be $\mu_\alpha = -60.2 \pm 4.9$ mas/yr and $\mu_\delta = -25.0 \pm 4.9$ mas/yr.

In order to assess the proper motion of 2M1207 without the effects of differential atmospheric refraction, another I-band image was obtained on 2006 July 8 (2006.52) at the Siding Spring Observatory 1 meter Telescope using the Wide Field Imager. A 480 second exposure was taken at airmass=1.06 (elevation 71 deg) with measured point source FWHMs= $1''.5$ (4

pixels). At this elevation, there should be negligible differential atmospheric refraction. Using the method described above against the 1978.33 epoch SuperCOSMOS image with 62 point sources in common, we calculate $\mu_\alpha = -61.0 \pm 4.6$ mas/yr and $\mu_\delta = -20.1 \pm 4.9$ mas/yr which is in good agreement with the analysis above.

A final proper motion value is estimated from the weighted average of the 1978/2005 and 1978/2006 epoch values: $\mu_\alpha = -60.6 \pm 3.4$ mas/yr and $\mu_\delta = -22.6 \pm 3.5$ mas/yr. The listed errors at each epoch are the scatter in field sources produced by GEOMAP. For a distance of 59 pc, the annual parallax of 2M1207 of 17 mas has negligible effect on our calculation because the 1978/2005/2006 measurements were obtained during similar seasons of the year. Furthermore, even for the worst case (17 mas offset for the 27 year baseline), this effect is much less than the random centroiding error.

4.2. Common proper motion pair

Measured separations between 2M1207 and 2M1207b from the HST and VLT are listed in Table 3. Due to the proper motion of the primary, relative positions between the primary and a stationary background object should change over time as illustrated in Figure 3. Because the 2004 Aug 28 HST observation has the best positional measurement accuracy, all other positions are plotted relative to it. If the planetary mass companion candidate seen in the 2004 Aug 28 image had been a stationary background source, then its position relative to 2M1207 would have changed along the black line of Figure 3. As clearly shown in Figure 3 and Table 3, 2M1207 and its planetary mass companion (2M1207b) are comoving, indicative of a gravitationally bound pair.

The weighted mean offset position of 2M1207b relative to 2M1207 from HST and VLT images is $\Delta\alpha = 629.8 \pm 1.3$ mas and $\Delta\delta = -448.1 \pm 1.1$ mas. Comparing this against the expected position for a background object at epoch 2005 Apr 26, $\Delta\alpha = 674.6 \pm 2.2$ mas, $\Delta\delta = -415.6 \pm 2.3$ mas, we find the two positions differ by 16.2σ . Using only the HST images, the level drops to 16.0σ which is an unambiguous independent confirmation of the proper motion companionship of 2M1207 and 2M1207b. Uncertainties in background object position were calculated using our improved proper motions and distance (59 pc, see Section 5 for details on distance estimation).

5. Discussion

Chauvin *et al.* (2005a) argue that the mass of 2M1207b falls in the planetary range

(< 13.6 M_J). To prove this conjecture one must establish that (1) 2M1207 is very young, i.e., a member of the ~ 8 Myr old TW Hydrae Association and (2) 2M1207 and 2M1207b are gravitationally bound.

Provided that (1) and (2) are true, then Chauvin et al (2004, 2005) describe how two, essentially independent, techniques – evolutionary modeling and surface gravity analysis – both yield masses for 2M1207b well below 13.6 M_J. In Figure 3 and Table 3 of the present paper, we establish with high confidence that 2M1207 and 2M1207b are gravitationally bound.

Thus, only membership of 2M1207 in the TWA remains to be considered. Chauvin et al. (2004) list a variety of reasons (their Section 3.1) why 2M1207 is a member of the TWA. We can now strengthen their argument. On-going Keck NIRSPEC spectroscopic surveys of brown dwarfs, both old and young, (e.g., McGovern 2005; McGovern *et al.* 2004; McLean *et al.* 2003) corroborate earlier measurements (mentioned in Chauvin *et al.* 2004) indicating low surface gravity in 2M1207, characteristic of ~ 10 Myr brown dwarf. Mohanty et al. (2005) report a detection of [O I] emission, which indicates a mass outflow from 2M1207, as well as a detection of accretion shock-induced UV emission (see their Section 5.1 for details). All these strongly support that 2M1207 is indeed a young accreting brown dwarf.

Using our new determination of the proper motion of 2M1207, we can derive a more reliable estimate of the distance to 2M1207 than was available to Chauvin et al. TWA members HR 4796A and 2M1207 lie very close together in the plane of the sky and, thus, should have proper motions which differ only according to their relative distances from Earth. The proper motion of HR 4796A is given in the Tycho 2 catalog ($\mu_\alpha = -53.3 \pm 1.3$ mas/yr, $\mu_\delta = -21.2 \pm 1.1$ mas/yr). We used Tycho-2 proper motions over published, ostensibly more precise, Hipparcos values because Hipparcos proper motion uncertainties seem to have been underestimated (e.g., Kaplan & Snell 2001 and Soderblom *et al.* 2005). From the ratio of total proper motions of HR 4796A and 2M1207 (1.144:1.000) and using the Hipparcos measured distance to HR 4796A (67.1 ± 3.4 pc), we deduce a distance to 2M1207 of 59 ± 7 pc. At this distance, the projected separation of 2M1207b from 2M1207 is 46 ± 5 AU.

Our proper motion based method to derive the distance to 2M1207 can be tested on TWA 25 which is also close in the plane of the sky to HR 4796A. The proper motion of TWA 25 is $(-75.9, -26.3)$, thus from the ratio of total proper motion to HR 4796A (1.400:1.000), one derives a distance to TWA 25 of ~ 48 pc. This is in good agreement with the photometric distance of 44 pc given in Song *et al.* (2003). In this case (unlike 2M1207), because TWA 25 is an M0 dwarf and there are many similar spectral type members in the TWA, the photometric distance should be fairly reliable. Thus, the agreement between the proper motion and photometrically derived distances for TWA 25, supports the proper

motion method we use to derive the distance to 2M1207.

Based on the moving cluster method, Mamajek (2005) estimated a somewhat smaller distance (53 ± 6 pc) to 2M1207. Because the moving cluster method to the TWA is grounded in good Hipparcos measured distances to only three stars (TW Hya, HD 98800, and HR 4796A; the Hipparcos distance to TWA 9 appears to be wrong), conclusions drawn in the study of Mamajek (2005) should be regarded with care. For example, that study rejects TWA membership for the nearby (~ 22 pc) mid-M dwarf TWA 22 (Song *et al.* 2003) because doing so substantially improves the vertex solution presented. Yet TWA 22 has a very strong lithium line (Song *et al.* 2003) and our survey of nearby, active, M-type stars over most of the sky (Song, Bessell, & Zuckerman, in preparation) has revealed strong lithium lines only in the direction of the TWA with the exception of a very few M-type members of the β Pic moving group. However, as the β Pic moving group has nearly the same Galactic space motion as the TWA (Table 7, Zuckerman & Song 2004), even in the very unlikely event that TWA 22 is a β Pic member, this could hardly impact the vertex solution. In addition, TWA 22 turns out to be a $\sim 0''.1$ binary with $\Delta K \sim 0.4$ mag (Chauvin et al., in prep.) pushing its photometric distance from 22 pc to 28 pc. Therefore, TWA 22 is very likely a true TWA member. Because of such issues, we adopt our 59 ± 7 pc distance determination for 2M1207, in preference to earlier estimations.

Calculations of opacity-limited fragmentation in a turbulent 3-D medium yield minimum masses $\gtrsim 7 M_J$ (e.g., Low & Lynden-Bell 1976; Boyd & Whitworth 2005; Bate 2005 and references therein). Given the uncertainties in these calculations and in evolutionary models of young, planetary-mass objects, our $5 \pm 3 M_J$ estimate for 2M1207b is likely not in conflict with the $7 M_J$ fragmentation mass. Alternatively, perhaps a different model, for example 2-D fragmentation of a shock compressed layer (Boyd & Whitworth 2005), will ultimately be needed to account for the properties of 2M1207b.

6. Conclusions

The common proper motion confirmation of the first imaged planetary mass companion to a celestial object other than our Sun enables the onset of a new era in extra-solar planet characterization – direct spectroscopic analysis. Absorption spectroscopy of stellar light reprocessed through atmospheres of planets detected through radial velocity surveys has been demonstrated (e.g., HD 209458b; Brown *et al.* 2001). 2M1207b provides the first opportunity to collect and spectroscopically analyze photons from an extra-solar planetary mass companion. Exploiting the superb stability of the HST, we will attempt to obtain a near-IR grism spectrum of 2M1207b. Relative to clear atmospheric models, dusty models

(Chabrier *et al.* 2000, for example) predict more flux suppression in the $1.0 - 1.3\mu\text{m}$ range, which can be readily compared to the anticipated $S/N \sim 10$ grism spectrum.

This research was supported by STScI through grant HST-GO-10176. Portions of this research were performed under the auspices of the U.S. Department of Energy by the University of California, Lawrence Livermore National Laboratory under Contract W-7405-ENG-48. We thank Michael Wenz (STScI) and Merle Reinhart (CSC) for their assistance in determining HST’s absolute orientation error following the guide star acquisitions for each of our orbits. Our gratitude is extended to Al Schultz and Beth Perrillo (our contact scientist and program coordinator at STScI) for their assistance in implementing and scheduling our observations. We thank Richard Crowe for kindly obtaining the 2005 *I*-band data and Bob Shobbrook for the 2006 *I*-band image used in our proper motion refinement. We thank a referee for pointing out to us the potential importance of differential atmospheric refraction in our 2005 *I*-band image.

REFERENCES

- Baraffe, I., Chabrier, G., Barman, T. S., Allard, F., & Hauschildt, P. H. 2003, *A&A*, 402, 701
- Bate, M. R. 2005, *MNRAS*, 363, 363
- Boyd, D. F. A. & Whitworth, A. P. 2005, *A&A*, **430**, 1059
- Brown, T. M., Charbonneau, D., Gilliland, R. L., Noyes, R. W., & Burrows, A. 2001, *ApJ*, **552**, 699
- Chabrier, G., Baraffe, I., Allard, F., & Hauschildt, P. 2000, *ApJ*, **542**, 464
- Chauvin, G., *et al.* 2004, *A&A*, **425**, L29
- 2005a, *A&A*, **438**, L25
- 2005b, *A&A*, **438**, L29
- Gizis, J. E. 2002, *ApJ*, 575, 484
- Gliese, W. 1969, *Veroeffentlichungen des Astronomischen Rechen-Instituts Heidelberg*, 22, 1

- Howell, S. B. 2000, *Handbook of CCD astronomy* / Steve B. Howell. Cambridge, U.K. ; New York : Cambridge University Press, c2000. (Cambridge observing handbooks for research astronomers ; 2)
- Kaplan, G. H., & Snell, S. C. 2001, *BAAS*, 33, 1493
- Kirkpatrick, J. D., Barman, T. S., Burgasser, A. J., McGovern, M. R., McLean, I. S., Tinney, C. G., & Lowrance, P. J. 2006, *ApJ*, 639, 1120
- Krist, J. E. & Hook, R. N. 1997, in *The 1997 HST Calibration Workshop with a New Generation of Instruments*, p. 192, 192
- Leggett, S. K., et al. 2002, *ApJ*, 564, 452
- Low, C. & Lynden-Bell, D. 1976, *MNRAS*, **176**, 367
- Lowrance, P. J., et al. 2000, *ApJ*, 541, 390
- Mamajek, E. E. 2005, *ApJ*, 634, 1385
- McGovern, M. R. 2005, *Ph.D. Thesis, UCLA*
- McGovern, M. R., et al. 2004, *ApJ*, **600**, 1020
- McLean, I. S., McGovern, M. R., Burgasser, A. J., Kirkpatrick, J. D., Prato, L., & Kim, S. S. 2003, *ApJ*, **596**, 561
- Mohanty, S., Jayawardhana, R., & Basri, G. 2005, *ApJ*, 626, 498
- Monet, D. G., Dahn, C. C., Vrba, F. J., Harris, H. C., Pier, J. R., Luginbuhl, C. B., & Ables, H. D. 1992, *AJ*, 103, 638
- Noll, K., et al. 2004, *NICMOS Instrument Handbook, Version 7*
- Schneider, G., et al. 2004, *BAAS*, 205, 1114
- Schneider, G., Silverstone, M. D., & Hines, D. C. 2005, *ApJ*, **639**, L227
- Scholz, R.-D., McCaughrean, M. J., Zinnecker, H., & Lodieu, N. 2005, *A&A*, **430**, L49
- Soderblom, D. R., Nelan, E., Benedict, G. F., McArthur, B., Ramirez, I., Spiesman, W., & Jones, B. F. 2005, *AJ*, 129, 1616
- Song, I., Zuckerman, B., & Bessell, M. S. 2003, *ApJ*, **599**, 342

Zuckerman, B. & Song, I. 2004, *ARA&A*, **42**, 685

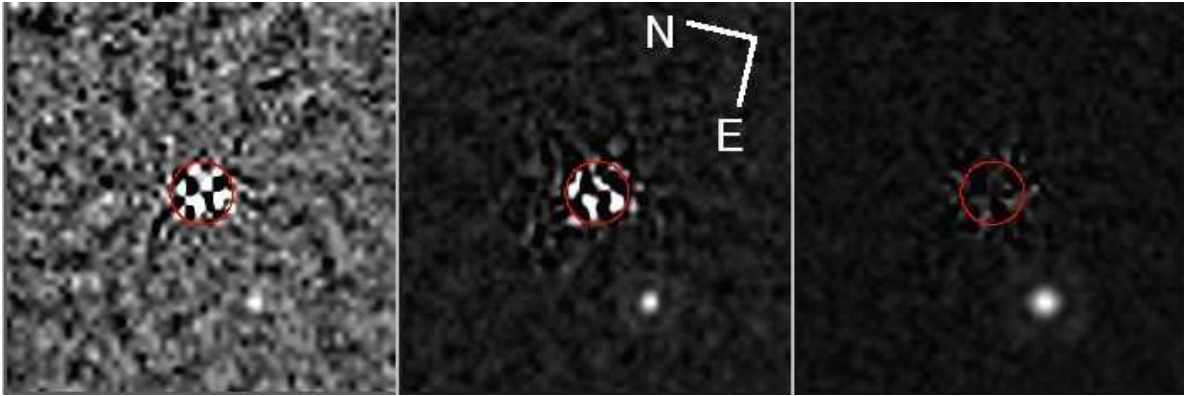


Fig. 1.— First epoch NICMOS camera 1 PSF-subtracted images of 2M1207 (centered in $0''.2$ radius circle) and its companion ($0''.77$ to the SE) at 0.9 , 1.1 , and $1.6 \mu\text{m}$ (left to right). By subtracting a second image of 2M1207 at a different celestial orientation, background light from the primary at the location of 2M1207b is effectively eliminated. Additionally, in each difference image, a flux-scaled, astrometrically-registered model PSF, fit to the “negative” image of 2M1207b, was added to eliminate the negative imprint from the difference image.

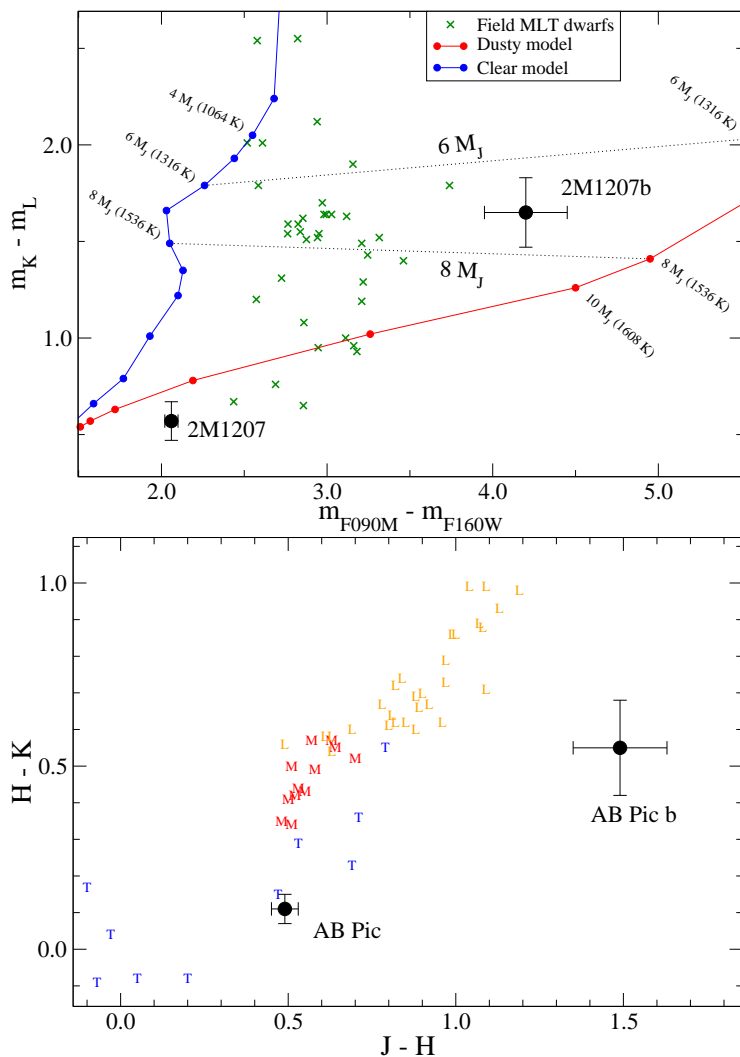


Fig. 2.— (a) NICMOS (from this study) and broadband (from Chauvin *et al.* 2004) colors of 2M1207 and 2M1207b are compared to “Dusty” (Chabrier *et al.* 2000) and “Clear” (Baraffe *et al.* 2003) models. F090M and F160W magnitudes of field M, L, & T dwarfs (Leggett *et al.* 2002) are calculated using the IRAF task SYNPHOT from their measured ground-based spectra. (b) Near infrared colors of AB Pic and b (Chauvin *et al.* 2005b) are compared to those of field M, L, & T dwarfs (Leggett *et al.* 2002). For both 2M1207b (L5 or later) and AB Pic b (L1), their extreme red color is caused by low surface gravity which is in turn attributed to their young ages. Figure 3 from Chauvin *et al.* (2004) shows a similar redness of 2M1207b in HKL' colors.

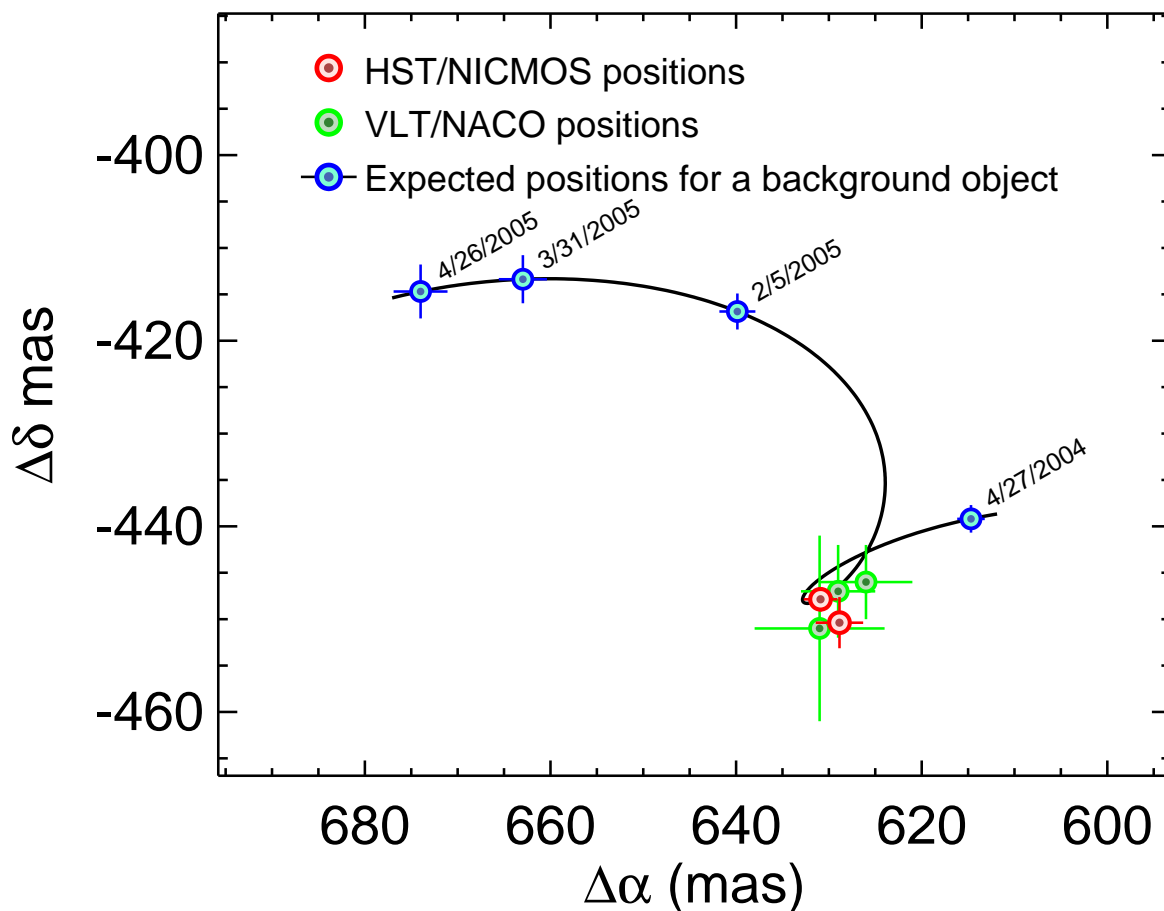


Fig. 3.— Unchanging separation and position angle between 2M1207 and 2M1207b. Observations with the HST and VLT prove that 2M1207 and its planetary mass companion share common proper motion, which means they are gravitationally bound. The green and red crosses mark the observed positions of the companion relative to 2M1207 on different dates. Were the planetary mass candidate seen in the 2004 Aug 28 image a stationary background object, then its position, relative to the position measured on 2004 Aug 28, would have changed as shown by the black line. A distance of 59 pc was used to calculate expected background positions.

Table 1: NICMOS Observations Summary

UT Date	2004 Aug 28			2005 Apr 26		
Orient ^a	279°:720/289°:620			187°:120/207°:120		
Filters	F090M	F110M	F160W	F090M	F145M	F160W
SAMPSEQ ^b	STEP64	STEP64	STEP8	STEP64	STEP64	STEP8
NSAMP ^c	13	12	12	13	12	12
EXPTIME ^d	2560s	2048s	448s	2560s	2048s	448s

^a Orientation angle of the image +Y axis east of north.

^b Multiaccum sample sequence (Noll *et al.* 2004).

^c Number of non-destructive readouts for each exposure.

^d Total exposure time for 4 filtered images at each orientation for each epoch.

Table 2. Photometry of 2M1207 and its companion.

		Filter	HST	HST
	Name	50% band pass (μm)	08/28/04 (mag)	04/26/05 (mag)
2M1207	F090M	0.80 – 1.00	14.66 \pm 0.03	14.71 \pm 0.04
2M1207	F110M	1.00 – 1.20	13.44 \pm 0.03	—
2M1207	F145M	1.35 – 1.55	—	13.09 \pm 0.03
2M1207	F160W	1.40 – 1.80	12.60 \pm 0.03	12.63 \pm 0.02
2M1207b	F090M	0.80 – 1.00	22.34 \pm 0.35	22.58 \pm 0.35
2M1207b	F110M	1.00 – 1.20	20.61 \pm 0.15	—
2M1207b	F145M	1.35 – 1.55	—	19.05 \pm 0.03
2M1207b	F160W	1.40 – 1.80	18.24 \pm 0.02	18.27 \pm 0.02

Note. — The uncertainties in the NICMOS magnitudes include error estimates from the model PSF fitting (companion) and aperture photometry (primary) as well as the uncertainties in the absolute photometric calibration of the instrument in each filter band for camera 1. Chauvin *et al.* (2004) reported JHKL' photometry of 2M1207 (J= 13.00 \pm 0.03 mag, H= 12.39 \pm 0.03 mag, K= 11.95 \pm 0.03 mag, & L' = 11.38 \pm 0.10 mag) and 2M1207b (H= 18.09 \pm 0.21 mag, K= 16.93 \pm 0.11 mag, and L' = 15.28 \pm 0.14 mag). The NICMOS F160W filter is \sim 30% wider than the ground-based Johnson H-band filters, so comparison of our data with previously published *H*-band data requires a careful conversion (see Lowrance et al. 2000, for details).

Table 3. Differential astrometry of 2M1207b relative to 2M1207.

	Epoch (UT)	Separation (mas)	Position Angle (deg E of N)	Instrument/Camera
2M1207b	28 Aug 2004	773.7 ± 2.2	125.37 ± 0.03	HST/NICMOS
2M1207b	26 Apr 2005	773.5 ± 2.3	125.61 ± 0.20	HST/NICMOS
2M1207b	27 Apr 2004	772 ± 4	125.4 ± 0.3	VLT/NACO
2M1207b	05 Feb 2005	768 ± 5	125.4 ± 0.3	VLT/NACO
2M1207b	31 Mar 2005	776 ± 8	125.5 ± 0.3	VLT/NACO
Weighted mean (HST + VLT)		773.0 ± 1.4	125.37 ± 0.03	
Field Star	28 Aug 2004	7795.3 ± 3.1	125.33 ± 0.01	
Field Star	26 Apr 2005	7848.9 ± 3.4	125.08 ± 0.06	

Note. — The uncertainties in the HST position measurements include known calibration errors in the NICMOS science instrument aperture frame, image centroiding, and the absolute error in the spacecraft orientation as determined from ancillary engineering telemetry downlinked from the HST pointing control system. Listed positions are for the F160W image centroids which are favored over other bands because; (a) they were identically observed in this highest S/N bandpass at both epochs, and (b) F160W PSFs ($\lambda/D \sim 0''.14$) are better sampled with the camera 1 pixel scale (43 mas/pixel) than the shorter wavelength observations. Positions were measured in all filter bands, and while all are consistent within their errors, the others are not quite as well determined as those made with F160W.